

# Lung Disease Classification Using Deep Learning

*Amruta Salagare*  
Dept CSE-AIML  
ATME College of Engineering  
Mysuru, India  
[amrutasalagare2609@gmail.com](mailto:amrutasalagare2609@gmail.com)  
*Afra Jabeen*  
Dept CSE-AIML  
ATME College of Engineering  
Mysuru, India  
[afrajabeen2508@gmail.com](mailto:afrajabeen2508@gmail.com)

*Reem K*  
Dept CSE-AIML  
ATME College of Engineering  
Mysuru, India  
[reemk3103@gmail.com](mailto:reemk3103@gmail.com)

*Anushree H M*  
Dept CSE-AIML  
ATME College of Engineering  
Mysuru, India  
[shreeanu218@gmail.com](mailto:shreeanu218@gmail.com)  
*Anil Kumar C J*  
Dept CSE-AIML  
ATME College of Engineering  
Mysuru, India  
[anilkumarcj@gmail.com](mailto:anilkumarcj@gmail.com)

**Abstract** – Lung diseases such as pneumonia, tuberculosis, and COVID-19 pose significant global health challenges due to high mortality rates and the critical need for timely, accurate diagnosis. Traditional diagnostic methods relying on manual interpretation of chest X-rays (CXR) are often time-intensive, inconsistent, and error-prone. This project introduces a deep learning-based system for automated multi-class classification of lung conditions, including pneumonia, tuberculosis, COVID-19, and normal lungs, using CXR images. The solution leverages a fine-tuned VGG19 model enhanced with custom layers, advanced data augmentation techniques, and transfer learning to optimize feature extraction, improve efficiency, and reduce computational costs. The architecture integrates Global Average Pooling, Dropout, and Dense layers to enhance regularization and scalability for real-time applications, while preprocessing and augmentation strategies ensure robustness against data quality variations. Achieving an accuracy of 96% with high precision, recall, and F1-scores across all classes, the system outperforms traditional diagnostic methods by addressing challenges such as high false-negative rates and limited generalizability. This automated tool offers a scalable, cost-effective, and efficient solution for clinical diagnostics, with potential for real-time deployment in resource-constrained settings. By transforming diagnostic workflows, it contributes to improved patient outcomes and advances global health management.

Keywords: CNN, chest X-ray, COVID-19, pneumonia, tuberculosis, VGG19

## I. INTRODUCTION

Lung diseases, such as pneumonia, tuberculosis, and COVID-19, are significant global health concerns, affecting millions annually with high mortality rates. Accurate and timely diagnosis is crucial for effective treatment and disease management. Chest X-rays (CXR) remain one of the most accessible and cost-effective

diagnostic tools, but traditional methods rely heavily on manual interpretation by radiologists[1], which can lead to inefficiencies and variability in results.

The advent of artificial intelligence (AI) and deep learning provides an opportunity to automate and enhance the diagnostic process, making it faster, more accurate, and less dependent on human expertise. This project introduces an innovative approach that leverages advanced deep learning models to classify chest X-ray images into four categories: pneumonia, tuberculosis, COVID-19, and normal lungs. By employing state-of-the-art architectures like Convolutional Neural Networks (CNNs) and transfer learning[4] with pre-trained models such as VGG-19, the system significantly improves classification accuracy and efficiency.

In this project, CNNs process chest X-ray images to extract disease-specific features, enabling precise classification. Transfer learning enhances the system's performance by leveraging knowledge from large, pre-trained datasets, thereby improving accuracy even with limited medical data. This automated diagnostic tool reduces reliance on manual interpretation, ensures rapid and consistent results, and provides a scalable, cost-effective solution for early disease detection. By transforming clinical practices, this approach has the potential to alleviate the global health burden of lung diseases and improve patient outcomes worldwide

## II. LITERATURE REVIEW

In the development of a deep learning model for lung disease classification using chest X-ray (CXR) images, various studies have made significant contributions to the methodologies and evaluation processes that informed the design of the model. Alshmrani et al. [1] developed a VGG19-based deep learning model, augmented with additional CNN layers, to improve feature extraction and classification accuracy for multiple lung diseases, including COVID-19, pneumonia, lung opacity, tuberculosis, and normal cases. The dataset used in their study was pre-processed with resizing, normalization, and

random splitting to optimize model training. The results achieved were impressive, with an accuracy of 96.48%, precision of 97.56%, recall of 93.75%, an F1 score of 95.62%, and a remarkable AUC of 99.82%. However, the study noted that the class imbalance within the dataset could affect model performance for underrepresented diseases. This insight emphasized the importance of dataset diversity and informed the decision to create a similar, diverse dataset for our model.

Shivanshu et al. [2] evaluated several CNN architectures, including DenseNet121, ResNet50, and VGG16, for classifying chest X-ray images of COVID-19, pneumonia, and tuberculosis. Their methodology involved stratified sampling to ensure balanced representation of various pulmonary diseases in the dataset, with data augmentation techniques to enhance model robustness and mitigate overfitting. Their results showed DenseNet121 and a custom CNN as the most effective models, achieving high accuracy and recall rates. ResNet50 and VGG16 also performed well but showed signs of overfitting after extended training. This study reinforced the value of using data augmentation and high-performance computing systems, which were key considerations in the development of our model.

In the domain of pneumonia detection, Kavitha et al. [3] compared various CNN architectures such as VGG19, Xception, DenseNet201, and Inception V3 for pneumonia detection in chest X-rays. They applied data enhancement techniques like contrast-limited adaptive histogram equalization and intensity normalization to improve feature visibility. Their approach also included employing UNET and cyclic GANs to augment limited COVID-19 data, improving the model's performance in classifying pneumonia and COVID-19 cases. Their findings, which demonstrated over 90% classification accuracy using MobileNetV2 and other specialized models, provided valuable insights for improving the classification of pneumonia and other lung diseases in our model.

Chouat et al. [4] employed transfer learning using pre-trained CNN models such as VGGNet-16 and MobileNet for classifying chest X-ray images into four categories: COVID-19, bacterial pneumonia, viral pneumonia, and normal cases. Their study showed that MobileNet outperformed VGGNet-16, achieving an accuracy of 82% and an AUC of 95%, while VGGNet-16 had an AUC of 94%. The study's success in using transfer learning techniques to classify lung diseases highlighted the efficacy of MobileNet in lung disease classification and led to its inclusion in our model.

Sultana et al. [5] evaluated the performance of EfficientNetB0, DenseNet169, and DenseNet201 in classifying lung diseases from chest X-rays. Using a dataset of 6,340 chest X-ray images, they applied preprocessing steps such as resizing, filtering, and augmentation. EfficientNetB0 achieved the highest accuracy of 99.15%, followed by DenseNet169 and DenseNet201 at 98.89% and 97.79%, respectively. Their results demonstrated the

efficacy of these models in lung disease classification and influenced our decision to incorporate EfficientNetB0, which provided high accuracy and robust performance for diverse lung conditions.

Finally, Kumar et al. [6] reviewed various deep learning models, including CNNs, LSTMs, and GANs, for medical image classification. The study highlighted the importance of diverse datasets and model robustness. The use of CNNs in combination with LSTMs for sequential data analysis, and the integration of GANs for data augmentation, pointed to new directions for future research. This comprehensive review provided a broad understanding of the deep learning techniques available for medical image classification, informing our approach to utilizing CNNs and exploring the potential of integrating additional deep learning techniques in future iterations of the model.

By combining the methodologies and results from these studies, the proposed deep learning model for lung disease classification benefits from a diverse set of techniques, including CNN architectures, transfer learning, data augmentation, and class balancing. These approaches collectively enhanced the model's accuracy and generalizability, ensuring its robustness across various lung diseases like COVID-19, pneumonia, tuberculosis, and normal condition

### III. METHODOLOGY

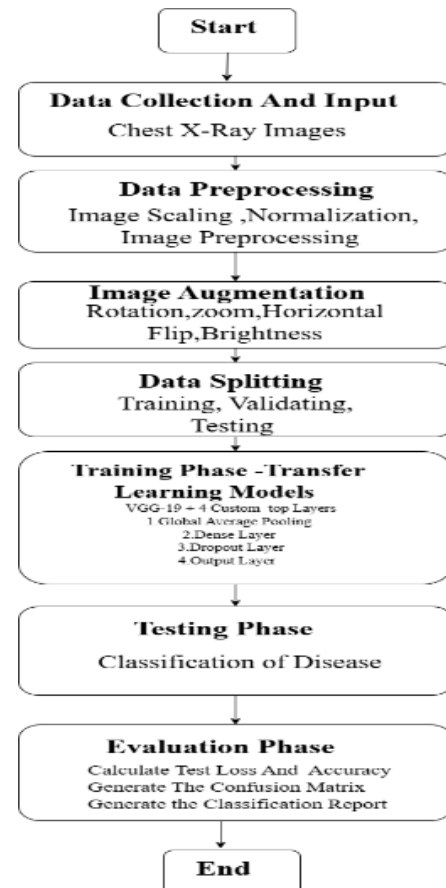


Fig 1: Flow Chart for the proposed Methodology

## A. Datasets

In this study, the dataset was sourced from Kaggle[20]. The data collection process aimed to ensure a comprehensive representation of pulmonary diseases, specifically tuberculosis (TB), COVID-19, and pneumonia. Dataset [19], sourced from a publicly available repository, consisted of chest X-ray images of individuals diagnosed with COVID-19, normal (non-diseased) individuals, and individuals with pneumonia. The dataset was composed of the following samples:

- COVID-19: 2031 images
- Normal: 1213 images
- Pneumonia: 2008 images
- Tuberculosis :2034 images

TABLE I  
DIVISION OF TARGET DATASET

Datasets	Covid-19	Normal	Pneumonia	Tuberculosis
Training	1218	1207	1204	1220
Validation	406	402	401	406
Testing	407	404	403	408

These images were carefully selected to represent different manifestations, severity levels, and variations in disease characteristics. The dataset encompassed diverse patient demographics, imaging techniques, and disease presentations.

A comprehensive collection of chest X-ray images was obtained, totaling 8086 samples. To ensure an equitable representation of each disease category in the training, validation, and testing subsets, a stratified sampling approach was employed.

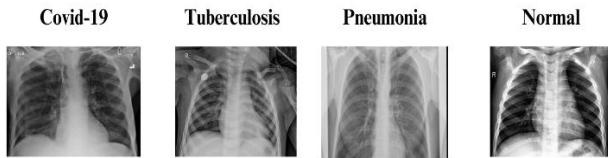


Fig : Sample of images taken from dataset.

## B. Data Preprocessing

In order to enhance the model's generalization capability, we employed a range of data preprocessing and augmentation techniques. To further improve the robustness of the model, various data augmentation methods were applied to the training data. These included random rotation of images up to 30 degrees to introduce orientation variability, as well as width and height shifting up to 20% of the image size to simulate positional variations. Additionally, random zooming within a range of 20% was performed to account for scale differences, and horizontal flipping was introduced to create mirrored variations of the images. Brightness adjustment was also incorporated, varying the brightness of images within a range of 80% to 120% to account for lighting conditions.

Finally, a fill mode was applied to handle missing areas in transformed images by using the nearest pixel values. These preprocessing and augmentation techniques were instrumental in creating a diverse and representative training dataset, thereby enhancing the model's ability to learn effectively and generalize across varied input scenarios.

## C. Proposed Model Creation

**Custom CNN :** The model is based on VGG19, a well-established pre-trained convolutional neural network, fine-tuned for the classification task using transfer learning to leverage its robust feature extraction capabilities. The VGG19 base model, initialized with pre-trained weights from ImageNet, was modified by removing the top fully connected layers and setting the input shape to 224X224 RGB channel image.

To retain the pre-trained features while enabling fine-tuning of deeper layers, all layers except the last four convolutional layers were frozen. Custom layers were then added, including a GlobalAveragePooling2D layer to reduce the feature map to a single vector for each filter, a dense layer with 256 neurons and ReLU activation, and a dropout layer with a rate of 0.5 to mitigate overfitting. Finally, the output layer was configured with 4 neurons and softmax activation for multi-class classification. This architecture effectively combines the pre-trained strengths of VGG19 with task-specific adaptations, ensuring accurate classification of input images.

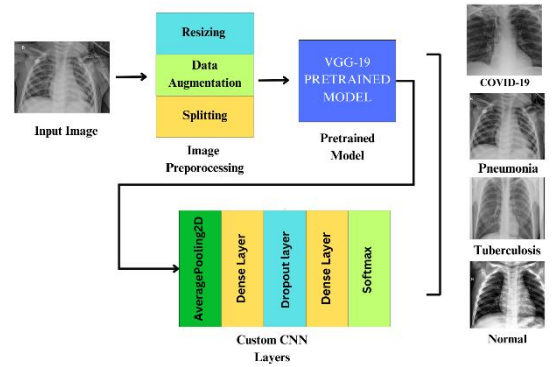


Fig 2 :Proposed Model Architecture

TABLE II  
PROPOSED CNN MODEL LAYERS ARCHITECTURE

Layer (Type)	Output Shape	Param #
VGG-19 Pretrained Convolutional layers	(None,7,7,512)	20,024,384
global_average_pooling	(None, 512)	0
Dense	(None, 256)	131,328
Dropout	(None, 256)	0
Output_layer	(None, 4)	1,028

## D. Hyper-parameters

**Batch Size:** Due to the memory limitations of RAM and the GPU's VRAM, the flexibility to experiment with different

batch sizes was restricted. As a result, a batch size of 32 was consistently used across all the trained models.

**Optimizer:** The Adaptive Momentum (Adam) optimizer was employed for training, as it is one of the advanced methods for effectively learning the model's weights.

**Learning Rate:** As the models utilized pre-trained weights through transfer learning for the convolutional networks, the learning rate was set to a low value of 0.0001 to ensure stable and efficient training.

**Activation Functions:** ReLU was used in all layers except the output layer to introduce non-linearity due to its simplicity and effectiveness. For the output layer, sigmoid activation was applied to handle the multi-label

**Loss Function:** Binary Cross-Entropy (BCE) ensures accurate evaluation for multi-label classification by treating each class independently, while Focal Loss addresses class imbalance by focusing on harder samples, ensuring balanced and robust model performance.

### E. Model Training

The proposed model was trained using the Adam optimizer, configured with a learning rate of  $1 \times 10^{-4}$ , known for its adaptability and effectiveness in gradient-based optimization tasks. To enhance computational efficiency, the training process used a batch size of 32 images, and the model was trained over a maximum of 20 epochs. Early stopping was implemented as a key strategy to mitigate overfitting. This technique monitored the validation loss during training and halted the process if no improvement was observed over five consecutive epochs, ensuring that the model preserved its generalizability. Additionally, the early stopping callback restored the best-performing weights from the training process.

After training, the finalized model, having demonstrated optimal performance, was saved for future use and deployment. This ensured that the trained model could be seamlessly integrated into applications or further fine-tuned for additional tasks.

### F. Model Evaluation

The evaluation of the proposed model began by analysing its training and validation performance through graphical representations of accuracy and loss. These graphs demonstrated the convergence of the model over the epochs, showcasing an upward trend in accuracy and a simultaneous reduction in loss for both the training and validation sets. This provided a clear visual confirmation of the model's learning efficiency and its ability to generalize effectively.

Subsequently, the model's classification performance was assessed using a confusion matrix. This matrix offered insights into the distribution of predictions across the four target classes, highlighting both correct predictions and misclassifications. The confusion matrix played a crucial

role in identifying specific areas where the model excelled and where it faced challenges. The four predicted findings of the confusion matrix are true positives (TP), false positives (FP), true negatives (TN), and false negatives (FN), which are required to generate the assessment criteria.

After obtaining the values of the confusion matrix, the following performance metrics were derived to evaluate the performance of the various pre-trained models employed.

**Accuracy:** As shown in eq (1), accuracy is equal to the sum of true positives and true negatives divided by the total values of the confusion matrix components. Accuracy: As shown in eq (1), accuracy is equal to the sum of true positives and true negatives divided by the total values of the confusion matrix components.

$$Accuracy = \frac{(TP+TN)}{(TP+TN+FP+FN)} \quad (1)$$

**Precision:** As shown in eq (2), precision is the portion of total number of samples anticipated to be positive and the number of samples that are really positive.

$$Precision = \frac{TP}{FP+TP} \quad (2)$$

**Recall:** Sensitivity or recall is defined as the ratio of the total number of correctly classified positive patients to the total number of positive patients, as shown in eq (3).

$$Recall = \frac{TP}{FN+TP} \quad (3)$$

**F1 score:** The proportional average of accuracy and recall is the F1 score. It is depicted in eq (4).

$$F1 \text{ score} = 2 \times \frac{precision \times recall}{precision+recall} \quad (4)$$

Finally, a detailed classification report was generated, providing key performance metrics for each class, including precision, recall, F1-score, and support. These metrics offered a comprehensive evaluation of the model's strengths and areas for improvement, ensuring a thorough understanding of its predictive capabilities. Collectively, these evaluation steps affirmed the reliability and robustness of the proposed model.

## IV. RESULT

The following results were captured after testing the model on the testing dataset, providing insights into its classification performance. Table II presents the evaluation metrics, including precision, recall, and F1-scores, achieved by the model on the testing data. The classes 0, 1, 2, and 3 in the table correspond to Covid-19, Normal, Pneumonia, and Tuberculosis, respectively. These metrics demonstrate the model's capability to effectively differentiate among these categories. Additionally, the graphical representation of the model's accuracy and loss trends during the training process is depicted in Figures III and IV, respectively. These graphs illustrate how the

model's performance improved over epochs, highlighting its ability to generalize well to unseen data and minimize errors during training.

TABLE III

PROPOSED CNN MODEL TESTING RESULTS.

Class	Precision	Recall	F1-score
0	0.97	0.98	0.97
1	0.92	0.97	0.94
2	0.97	0.91	0.94
3	0.98	0.98	0.98

Table II provides a detailed evaluation of the custom CNN model's classification performance for the four classes: Covid-19, Normal, Pneumonia, and Tuberculosis. The model achieves exceptional precision, recall, and F1-scores, with Covid-19 and Tuberculosis classes showing the highest reliability, attaining F1-scores of 0.97 and 0.98, respectively. The Normal and Pneumonia classes also exhibit commendable performance, both achieving F1-scores of 0.94. However, there is a slight variation in precision and recall for these categories, indicating minor misclassifications that can be further optimized. Overall, the results highlight the model's robust capability in accurately distinguishing among the four classes, demonstrating its potential for real-world deployment in lung disease classification tasks.

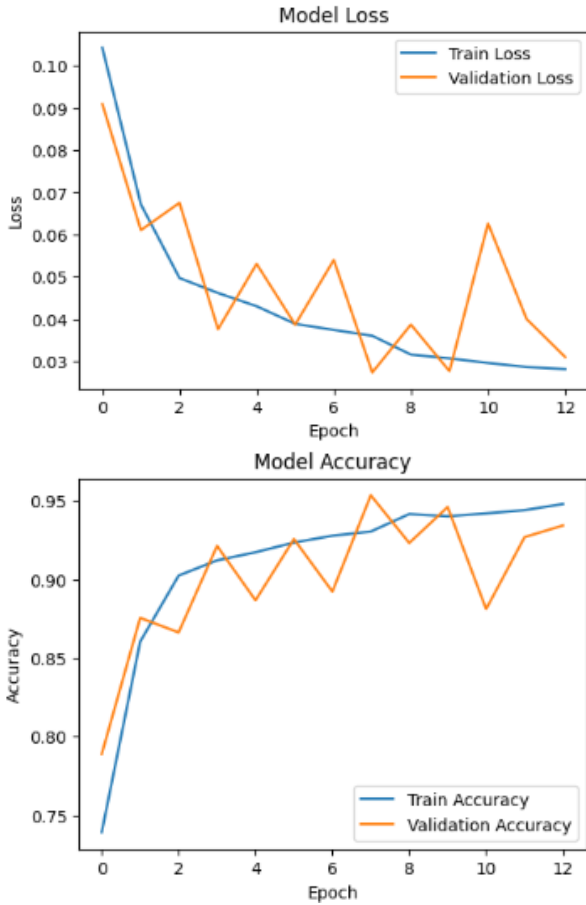


Fig 3: Loss and accuracy values for training and validation sets during training

The training accuracy increased significantly, reaching approximately 96.09%, while the validation accuracy achieved 95.36% by the final epoch. Concurrently, the training loss decreased to 0.01, and the validation loss reduced to 0.03, reflecting the model's ability to generalize effectively to unseen data. Early stopping was triggered at epoch 12 (from an initial limit of 20 epochs) to prevent overfitting, ensuring the model's optimal performance on the validation set.

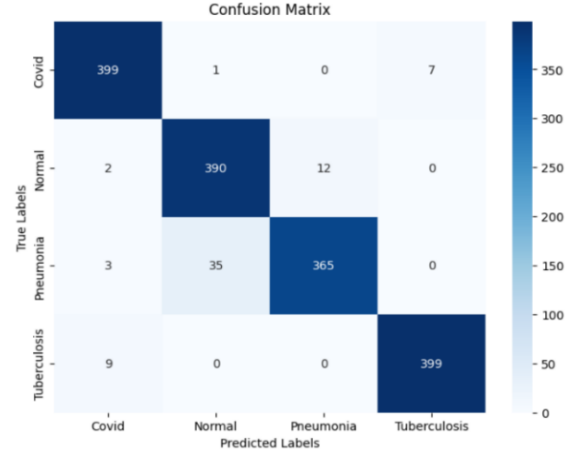


Fig 4: The confusion matrix of lung dataset

The confusion matrix illustrates the performance of the model across the four classes: Covid-19, Pneumonia, Tuberculosis, and Normal. For Covid-19, the model correctly classified 399 out of 409 instances. However, it misclassified 1 instance as Normal and 7 instances as Tuberculosis. For Normal, the model correctly classified 390 out of 404 instances, with 2 instances misclassified as Covid and 12 as Pneumonia. In the case of Pneumonia, the model correctly identified 365 out of 403 instances but misclassified 3 instances as Covid and 35 instances as Normal. Finally, for Tuberculosis, the model correctly classified 399 out of 408 instances, with 9 instances misclassified as Covid.

TABLE IV  
PROPOSED CNN MODEL RESULTS.

Model	Training Accuracy	Validation Accuracy	Testing Accuracy
Custom VGG-19	96.09	95.36	95.75

## V. CONCLUSION

The deep learning model, leveraging VGG-19 as a baseline and custom layers, achieved an overall accuracy of 95.62%, demonstrating its robust ability to classify chest X-ray images into four categories: Normal, COVID-19, Pneumonia, and Tuberculosis. This high accuracy reflects the effectiveness of the model in handling complex medical imaging tasks.

The model performed exceptionally well in classifying COVID-19 cases, achieving a precision of 97.34%, recall of 97.56%, and an F1-score of 97.45%, showcasing its ability to accurately detect this critical category. For Tuberculosis, the model achieved the highest metrics among all categories, with a precision of 98.27%, recall of 97.80%,



and an F1-score of 98.03%, highlighting its reliability in identifying this disease.

For Normal cases, the model displayed solid performance with a precision of 91.37%, recall of 96.54%, and an F1-score of 93.89%, reflecting its capability to distinguish healthy lungs. In the case of Pneumonia, the model achieved a precision of 96.83%, recall of 90.57%, and an F1-score of 93.58%, further indicating its competence in diagnosing this condition.

Overall, the combination of transfer learning with custom fine-tuning and advanced techniques like data augmentation and Focal Loss contributed to the model's high performance. These results validate the model's potential as a valuable tool in the classification of pulmonary diseases using chest X-ray images, paving the way for its application in clinical decision-making and further improvements in the future.

## VI. FUTURE SCOPE

Future research can focus on enhancing the **interpretability** of the deep learning model by incorporating techniques like **Gradient-weighted Class Activation Mapping (Grad-CAM)**. Grad-CAM helps visualize the regions of the chest X-ray (CXR) images that are most influential in the model's predictions. This visual feedback will provide **radiologists** with a clearer understanding of how the model arrives at its conclusions, improving transparency and fostering greater trust in its decision-making process. By offering insights into the specific areas of the image that contribute to the classification, this interpretability enhancement could help radiologists confidently collaborate with the system, making the diagnostic process more reliable and clinically valuable.

Additionally, the model's applicability can be expanded by incorporating **diverse datasets** to classify a broader spectrum of **pulmonary diseases**, including rare and less common conditions. By leveraging more comprehensive datasets, the model can improve its **generalizability** and **robustness**, ensuring it performs effectively across a wider range of **medical conditions**.

This approach would not only enhance the model's capability to handle diverse patient populations but also make it more versatile in various clinical environments. With such expansions, the system can contribute to **early detection** and more accurate diagnosis across multiple disease types, ultimately improving **patient outcomes** in diverse healthcare settings.

## VII. REFERENCES

- [1] G. M. M. Alshmrani, Q. Ni, R. Jiang, H. Pervaiz, and N. M. Elshennawy, "A deep learning architecture for multi-class lung diseases classification using chest x-ray (cxr) images," *Alexandria Engineering Journal*, vol. 64, pp. 923–935, 2023. [Online]. DOI: <https://www.sciencedirect.com/science/article/pii/S1110016822007104>
- [2] Shivanshu, R. Bisht, K. Mittal and G. P. M. S, "Evaluation of CNN Models for Accurate Classification of COVID-19, Pneumonia, Tuberculosis in Chest X-ray Images," 2023 3rd Asian Conference on Innovation in Technology (ASIANCON), Ravet IN, India, 2023, pp. 1-6, DOI: [10.1109/ASIANCON58793.2023.10270526](https://doi.org/10.1109/ASIANCON58793.2023.10270526)
- [3] K. S, R. S. Shudapreyaa, P. Prakash, V. S, V. V and Y. S, "Classification of Lung Diseases Using Transfer Learning with Chest X-Ray Images," 2024 Second International Conference on Emerging Trends in Information Technology and Engineering (ICETITE), Vellore, India, 2024, pp. 1-6, DOI: [10.1109/ic-ETITE58242.2024.10493367](https://doi.org/10.1109/ic-ETITE58242.2024.10493367)
- [4] Chouat, A. Echtioui, R. Khemakhem, W. Zouch, M. Ghorbel and A. B. Hamida, "Lung Disease Detection in Chest X-ray Images Using Transfer Learning," 2022 6th International Conference on Advanced Technologies for Signal and Image Processing (ATSIP), Sfax, Tunisia, 2022, pp. 1-6, DOI: [10.1109/ATSIP55956.2022.9805892](https://doi.org/10.1109/ATSIP55956.2022.9805892)
- [5] S. Sultana, A. Pramanik and M. S. Rahman, "Lung Disease Classification Using Deep Learning Models from Chest X-ray Images," 2023 3rd International Conference on Intelligent Communication and Computational Techniques (ICCT), Jaipur, India, 2023, pp. 1-7, DOI: [10.1109/ICCT56969.2023.10075968](https://doi.org/10.1109/ICCT56969.2023.10075968)
- [6] Kumar, R., Kumbharkar, P., Vanam, S. et al. Medical images classification using deep learning: a survey. *Multimed Tools Appl* 83, 19683–19728 (2024). DOI: <https://doi.org/10.1007/s11042-023-15576-7>
- [7] Yadav, S.S., Jadhav, S.M. Deep convolutional neural network based medical image classification for disease diagnosis. *Journal of Big Data* 6, 113 (2019). DOI: <https://doi.org/10.1186/s40537-019-0276-2>
- [8] O. Yadav, K. Passi and C. K. Jain, "Using Deep Learning to Classify X-ray Images of Potential Tuberculosis Patients," 2018 IEEE International Conference on Bioinformatics and Biomedicine (BIBM), Madrid, Spain, 2018, pp. 2368-2375, DOI: [10.1109/BIBM.2018.8621525](https://doi.org/10.1109/BIBM.2018.8621525)
- [9] O. A. Alrusaini, "Covid-19 detection from x-ray images using convoluted neural networks: A literature review," *International Journal of Advanced Computer Science and Applications*, vol. 13, no. 3, p. 78 – 88, 2022, cited by: 3; All Open Access, Gold Open Access.
- [10] Ouyang X, et al. Dual-sampling attention network for diagnosis of COVID19 from community acquired pneumonia. *IEEE Trans Med Imaging*. 2020;39(8):2595–605. <https://doi.org/10.1109/TMI.2020.2995508>
- [11] M. Hassouna, M. Al-Antary, M. Saleh and N. B. Al Barghuthi, "Applications of Deep Learning in Medical Imaging: A Brief Review," 2023 Advances in Science and Engineering Technology International Conferences (ASET), Dubai, United Arab Emirates, 2023, pp. 1-4, DOI: [10.1109/ASET56582.2023.10180645](https://doi.org/10.1109/ASET56582.2023.10180645)
- [12] M. Irtaza, A. Ali, M. Gulzar and A. Wali, "Multi-Label Classification of Lung Diseases Using Deep Learning," in *IEEE Access*, vol. 12, pp. 124062-124080, 2024, DOI: [10.1109/ACCESS.2024.3454537](https://doi.org/10.1109/ACCESS.2024.3454537)
- [13] JM. Berrimi, S. Hamdi, R. Y. Cherif, A. Moussaoui, M. Oussalah and M. Chabane, "COVID-19 detection from Xray and CT scans using transfer learning," 2021 International Conference of Women in Data Science at Taif University (WiDSTaif ), Taif, Saudi Arabia, 2021, pp. 1-6, DOI: [10.1109/WiDSTaif52235.2021.9430229](https://doi.org/10.1109/WiDSTaif52235.2021.9430229)
- [14] Ashwini, S., Arunkumar, J.R., Prabu, R.T. et al. Diagnosis and multi-classification of lung diseases in CXR images using optimized deep convolutional

- neural network. *Soft Comput* 28, 6219–6233 (2024). DOI: <https://doi.org/10.1007/s00500-023-09480-3>
- [15] Patil,P.,Narawade, V. RESP dataset construction with multiclass classification in respiratory disease infection detection using machine learning approach. *Int. j. inf. tecnol.* (2024). DOI: <https://doi.org/10.1007/s41870-024-01851-9>
- [16] R.S.Gargees, "Multi-Class Flat Classification of Lung Diseases Utilizing Deep Learning," 2022 IEEE IAS Global Conference on Emerging Technologies (GlobConET), Arad, Romania, 2022, pp. 804-809, DOI: [10.1109/GlobConET53749.2022.9872480](https://doi.org/10.1109/GlobConET53749.2022.9872480)
- [17] G. R. Khanaghavalle, A. Manoj, J. Karthikeyan and R. Murali, "A Deep Learning Framework for Multiclass Categorization of Pulmonary Diseases," 2023 World Conference on Communication & Computing (WCONF), RAIPUR, India, 2023, pp. 1-6, DOI: [10.1109/WCONF58270.2023.10235057](https://doi.org/10.1109/WCONF58270.2023.10235057)
- [18] ] M. R. Santhoosh, V. Praveen, A. M. Riyaz, M. Selvam Narendiran,R.V.Vibhinarayananand B. Prabha, "Classification of Lung Disease with Recommendation using Deep Learning," 2024 International Conference on Cognitive Robotics and Intelligent Systems (ICC - ROBINS), Coimbatore, India, 2024, pp.120-126, DOI: [10.1109/ICC-ROBINS60238.2024.10533947](https://doi.org/10.1109/ICC-ROBINS60238.2024.10533947)
- [19] <https://www.kaggle.com/datasets/amrutasalagare/lung-disease-dataset>
- [20] <https://www.kaggle.com/datasets/omkarmanohardalvi/lungs-disease-dataset-4-types>
- [21] <https://www.geeksforgeeks.org/vgg-net-architecture-explained/>
- [22] [https://en.wikipedia.org/wiki/Neural\\_network\\_\(machine\\_learning\)](https://en.wikipedia.org/wiki/Neural_network_(machine_learning))
- [23] ]<https://www.engati.com/glossary/softmax-function>